

Experimental Study of Corrosion on A36 Mild Steel Towards Aqueous 2-Amino-2-Ethyl-1, 3-Propanediol and Diethanolamine

Sami Ullah, M .A. Bustam, A. M. Shariff*, Girma Gonfa, M. Ayoub, M. Raihan

Research Center For CO₂ Capture, Chemical Engineering Universiti Teknologi PETRONAS, 32610, Bandar Seri Iskandar, Perak Malaysia

*E-mail: azmish@petronas.com.my

Received: 20 June 2016 / Accepted: 9 December 2016 / Published: 30 December 2016

Carbon dioxide (CO₂) absorption is a very promising approach to reduce CO₂ emissions from different industries especially power plants and then transport to injection sites. Then it passes through sequestration process for long-term storages that have a variety of suitable geologic formations. CO₂ absorption dealing with a wide range of amine solutions that are mostly used for this purpose. Additionally, most of the amine solutions are corrosive in nature, either they are lean or saturated with CO₂. In the present work, this corrosive behavior of 2- amino-2-ethyl-1, 3-propanediol (AEPD) and Diethanolamine (DEA) towards A36 mild steel have been investigated through the weight loss and electrochemical methods. The latest techniques like Field Emission Scanning Electron Microscopy (FESEM) and Energy-Dispersive X-ray (EDX) have been used for surface analysis of mild steel after corrosion test. Three different aqueous concentration of AEPD, DEA, and blended mixtures (0.3M, 0.6M, 0.9M) have been studied to determine the corrosion rate on mild steel. The effects of temperature and concentration on this process have been carried out by using electrochemical corrosion measurement techniques. The aqueous DEA with a concentration of 0.9M at 50°C resulted much higher corrosion rate (337.721×10^{-3} mm/year) compare to corrosion rate (35.867×10^{-3} mm/year) of 0.9M AEPD. The corrosion yield of a blended mixture of AEPD and DEA with 0.9M concentration was noted 119.115×10^{-3} mm/year.

Keywords: Corrosion rate; 2-amino-2-ethyl-1, 3-propanediol (AEPD); Diethanolamine (DEA); Mild steel; Amine;

1. INTRODUCTION

Intensive human activities and economic development have been contributing a significant rise in the concentration of greenhouse gases since last decade. A major component, Carbon dioxide (CO₂) is mainly emitted from fossil fuels for example coal and oil, used for producing energy, its emissions came from many types of industrial processes which are related to the oil refineries, natural gas, post combustions, cement and iron production [1-5]. CO₂ capture has attracted great interest now a day due

to its releases are supporting to global climate change and it is critical to advance the technologies to alleviate this problem. CO₂ absorption is a very promising approach to reduced CO₂ emissions.

Currently, a wide range of amine solutions are mostly used for CO₂ absorption process [6, 7]. CO₂ absorption method using aqueous amine solution has faced corrosion problems in many plants [8-13]. As quite a large number of equipment and pipeline in the amine, plants are made of carbon steel [14-16] which are corroded by amine solutions. Industrially, alkanol amines are more often used for gas absorption process for CO₂ absorption [17, 18]. Among them are monoethanolamine (MEA), Diethanolamine (DEA), N-methyldiethanolamine (MDEA), 2-amino-2-methyl-1-propanol (AMP), and others [19-27]. DEA plants generally experience less corrosion than MEA plants, but corrosion is also a concern for DEA plants and others [28-31]. Choice of certain amines depends on the absorption ability [32, 33], reaction kinetics [34-36], reformative potential and capacity [37]. However, that conventional alkanolamine contained some disadvantages, such as high solvent regeneration costs, high corrosion activities taking place in the pipelines [38, 39].

The corrosion rate in the CO₂ absorption system can be improved by sterically hindered amines (SHA). SHA refers to a new type of amine which is derived from the conventional amine by the addition of another functional group such as methyl and hydroxyl [40]. The addition of these functional groups will create a steric effect which can improve the absorption capability of the amine. Steric effect refers to the fact that each atom within a molecule occupies a certain amount of spaces. Sterically hindered amines produce unstable carbamates due to the obstacle of the bulky group neighboring to the amino group, and, therefore, provide more amine molecules to absorb CO₂. Considerably, higher reaction kinetics relative to tertiary amines, combined thru low solvent regeneration cost provides SHA with significant industrial benefits for CO₂ absorption [41, 42].

To minimize corrosion by taking into account of the emerging SHA, 2- amino-2-ethyl-1, 3- propanediol (AEPD) has been chosen, due to the high uptake in CO₂ absorption and stable form of carbamate formed during the reaction with CO₂ [24].

The usage of mixed/blended alkanolamine has come to be very appealing, as the mixture of individually amine benefit, such as fast reaction kinetics from a primary or secondary alkanolamines (e.g, DEA) consisted of increased absorption capability and reduce the solvent regeneration cost from a tertiary or sterically hindered alkanolamines [43, 44]. The corrosion of AEPD and blended solution of AEPD and DEA have not been reported in the literature.

The objectives of this research work are to determine the corrosion rate of mild steel in an aqueous solution of AEPD and DEA at 50°C by using weight loss method. The effects of concentration and temperature on aqueous AEPD and DEA was carried out by using the electrochemical method. Furthermore, the corrosion rates of blended amines of AEPD and DEA (0.3M, 0.6M, 0.9M) at 50°C were determined. The morphology and Energy-Dispersive X-ray (EDX) of mild steel corroded surface samples were examined for corrosion products.

2. EXPERIMENTAL

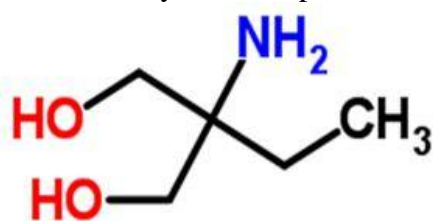
2.1. Materials

AEPD with a 97% purity was purchased from Acros Organics and was used without further

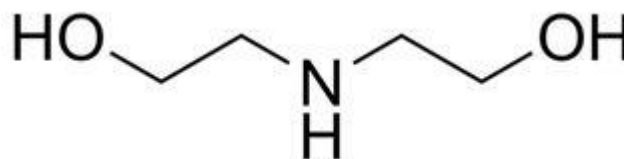
purification. Diethanolamine (DEA) was bought from Merck. A36 mild steel plate having weight composition (wt. %) C = 0.20, Mn = 0.45, Si = 0.31, S = 0.006, P = 0.04 and balance Fe was delivered by TSA Industries (Ipoh) Sdn. Bhd. Malaysia.

2.2. Preparation of Amine Solutions

Three different concentrations of AEPD have been prepared 0.3, 0.6 and 0.9M using the degassed triple-distilled water, and effect of concentration and effect of temperature have been carried out. Another three different concentrations of DEA 0.3, 0.6, 0.9M have been prepared to study the corrosion rate at 50°C. Furthermore, three different blended solutions of AEPD and DEA have been prepared 0.3, 0.6 and 0.9M concentration to study the corrosion rate at 50°C. The chemical structures of 2-Amino-2-Ethyl-1, 3-Propanediol and Diethanolamine are given below.



2-Amino-2-Ethyl-1, 3-Propanediol (AEPD)



Diethanolamine

2.3. Weight loss experiment

The mild steel samples were entirely immersed in 30 ml of amine solutions in corrosion cell. The immersion tests were carried out at 50°C for 30 days. Subsequently 24 hours, the samples were introverted, scrubbed using 20% (w/v) NaOH with zinc dust powder in order to remove the corrosion products. The samples were washed with distilled water and acetone, then dried and weighed. The test was executed three times and average values are used to calculate the corrosion rate.

2.4. Corrosion Rate

The corrosion rate per year (mmpy) was calculated using the following equation (1) according to [45].

$$CR = \frac{8.76 \times 10^4 w}{\rho A t} \quad (1)$$

where; CR (mm/year) is corrosion rate, w (g) is the weight loss of the mild steel specimen, ρ is density (g/cm^3), A (cm^2) is the total surface area of the specimen, and t (h) is the immersion time.

2.5. Electrochemical measurements

Electrochemical measurements were attained so as to validate the results of weight loss measurement. Mild steel was expurgated using an abrasive cutter to the dimension of 19x16 mm. Steel

samples have been mounted in epoxy and hardener with 5:1 ratio to approximately justified space by using aluminum foil and samples were dried for 24 hours. One side of the mild steel samples was ground to expose and polished for corrosion test. Measure the area of exposed mild steel for further measurements. The electrochemical tests were implemented out in a three-electrode corrosion cell for the quantitative examination of mild steel corrosion. The working electrode is the steel sample which is intended to observe and measure the corrosion rate. Current measurements could be changed into current densities for further analysis and calculation. The counter/auxiliary electrode is the name specified for the second electrode which is extant precisely to transmit the current in the circuit formed by the observations. The third electrode is called “reference electrode” and is existent to deliver exact steady datum point across the potential of the working electrode that can be deliberate. Other essential components needed for the experiment is a source of the potential, current and potential device. A solution of amine poured into the corrosion cell container, and the all the electrodes are immersed in it. The wires are connected to the corrosion cell, and the equipment is connected to the WEIS software which is installed on the connected computer. Tafel Plot results obtained from WEIS software. The trend of the plot is observed for every trial, and other parameters such as voltage, current, are also monitored. The result from WEIS is exported into IVMAN software which is used for Tafel analysis for corrosion rate and corrosion coefficients.

The specimens were cleaned with acetone and washed with distilled water and dried. The tests were performed in three-electrode glass cell assembly with graphite used as a counter electrode, Ag/AgCl as a reference electrode and A36 mild steel as working electrode. The corrosion cell is placed in an oil bath to control the temperature. The experimental were carried out at three different temperature 50°C, 70°C, 90°C. Moreover, to study the influence of different blended solutions of AEPD and DEA corrosivity towards mild steel 0.3, 0.6 and 0.9M concentration at 50°C. The Tafel, potentiodynamic polarization curves were obtained for each specimen at different concentration and temperature. The corrosion rate was calculated by using the following equation (2).

$$CR = \frac{0.13 \times I_c \times E_w}{A \times D} \quad (2)$$

I_c is corrosion current (microamperes per square centimeters), E_w is equivalent weight of the specimen (grams), in this experiment = 27.92g. A is the surface area of the specimen (squared centimeters), in this experiment = 0.54 cm², D is the density of the specimen (grams per centimeter cube), in this experiment = 7.95 g/cm³, CR - corrosion rate, measured in millimeter per year (mmpy).

2.6. Field Emission Scanning Electron Microscopy (FESEM)

Zeiss Sigma FESEM and EDX have been used for the surface analysis of corrosion products on the surface of mild steel after corrosion test.

3. RESULTS AND DISCUSSION

3.1. Weight loss measurements

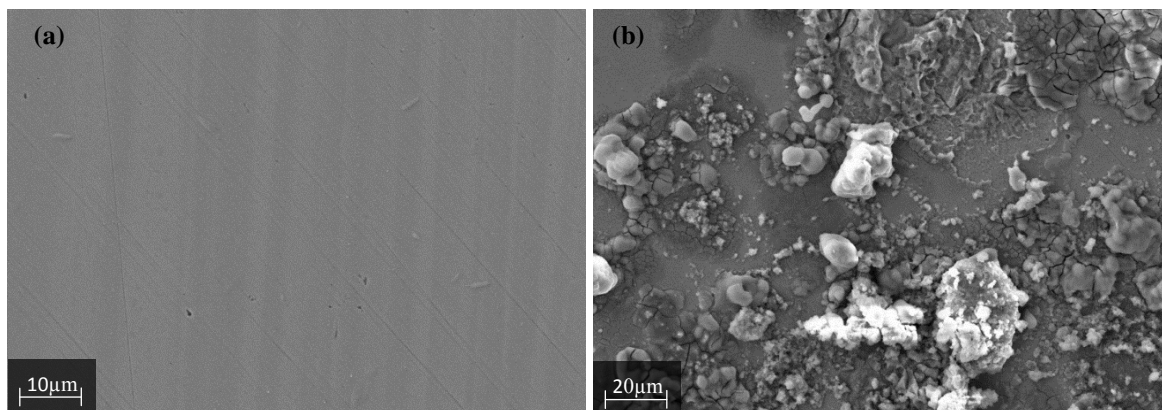
The corrosion rates of A36 mild steel in AEPD and DEA were gained from weight loss experiment under precise environments at 50°C are presented in Table 1. The estimated corrosion rate of DEA was 7 times higher than AEPD. These results showed that diethanolamine is more corrosive than sterically hindered amines.

Table 1. Corrosion rate of mild steel in AEPD and DEA with 0.9M at 50°C

<i>Concentration</i>	<i>Immersion time (h)</i>	<i>CR [mmpy]×10⁻³</i>
0.9M AEPD	720	51.350
0.9M DEA	720	364.575

3.2. Surface Analysis

FESEM has been used for surface structure analysis of tested steel samples. The first sample is the A36 mild steel which was immersed in 0.9M solution of AEPD at 50°C. The second sample is the A36 mild steel was immersed in 0.9M DEA solution at 50°C. Figure 1(a) showed the image of A36 mild steel as controlled sample before it dunked in the amine solution. From Figures 1 (b, c), FESEM images showed the pattern of corrosion on the steel and EDX results are presented in Table 2. Roughly at lower magnification, it showed the images of holes on the surface of the metal. At higher magnification, it showed a clear view, in which it displays observable images of cracks, signifying that the corrosion of the steel has been taken place and destroyed the structure. The results showed that the surface of sample are damaged after being baptized in the aqueous amine media. It also indicates serious corrosion attack on the steel sample and cracked the specimen's surface. Corrosion taking place in the deepest polished line, where amine droplets were more easily retained. The corrosion products established at certain local surface areas due to amine droplets retained on the surface. EDX results showed the element compositions that exist on the scanned surface of corroded specimen as given in Figure 2. Fe being the major component that is recorded and the composition of all elements found by the scan are presented in Table 2.



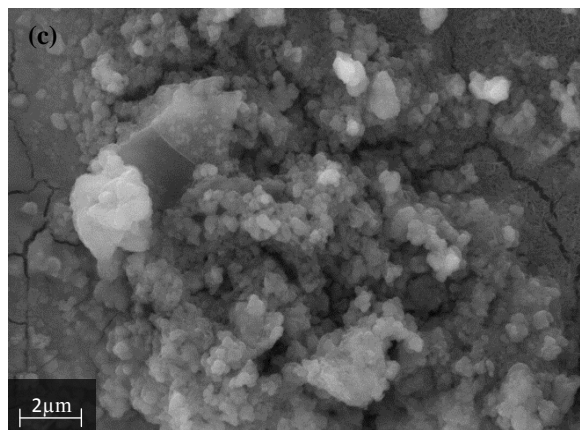


Figure 1. FESEM images of mild steel sample before corrosion test (a), Corrosion products and cracks (a, b) on the mild steel samples after corrosion test in 0.9 M of AEPD at 50 °C

Table 2. Elements Found on the Scanned Sample 1

Element	Weight (%)	Atomic (%)
Carbon, C	10.08	23.05
Oxygen, O	26.63	45.69
Chlorine, Cl	0.55	0.42
Iron, Fe	62.74	30.84

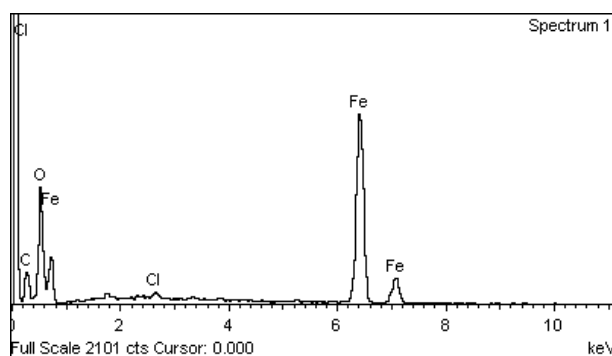


Figure 2. Energy-Dispersive X-ray (EDX) spectrum of the mild steel after corrosion test

From Figure 3 (a, b, c), the second sample was observed several parts of the steel show the corrosion that has been taken place. FESEM microstructure shows an irregular porosity structure of corrosion on the surface of steel sample is due to penetration of corrosive elements to the metallic substrate. The DEA formed slack corrosion products which permitted a prompt diffusion rate of the corrosive substance and consequently, higher corrosion rates were found. Ferrite microstructure is formed at the sample surface, looks more obvious compared to the AEPD sample. The corrosion products are formed in a systematic structure. Element composition that exists on the scanned surface, with iron being the major component that is recorded in EDX analysis as illustrated in Table 3 and Figure 4. The oxygen and chloride identified on the surface of the samples are due to the development

of corrosion products. These results show that AEPD delivers a less active surroundings for carbon steel compare to the DEA.

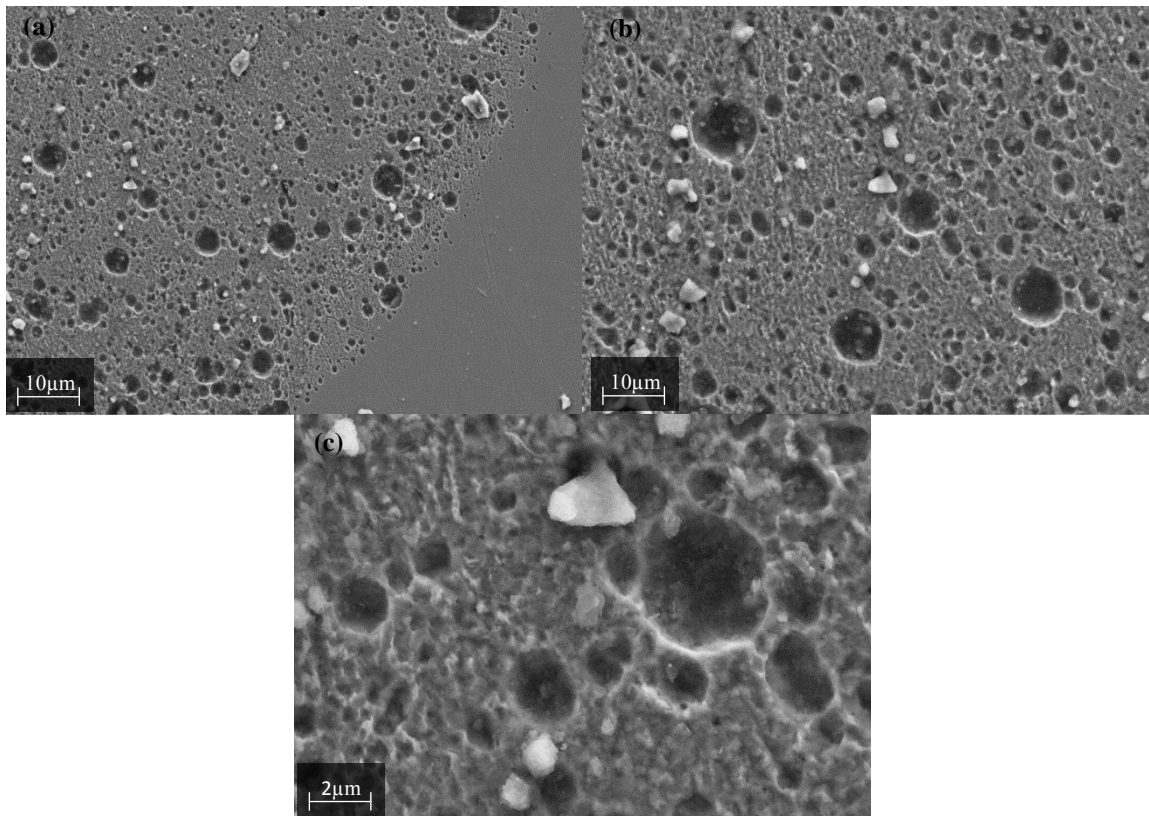


Figure 3. FESEM images of the mild steel samples (a, b, c) after corrosion test in the 0.9 M DEA at 50°C

Table 3. Elements Found on the Scanned Sample 2

Element	Weight (%)	Atomic (%)
Carbon, C	6.13	16.93
Oxygen, O	8.20	21.30
Chlorine, Cl	0.46	0.43
Iron, Fe	85.21	61.34

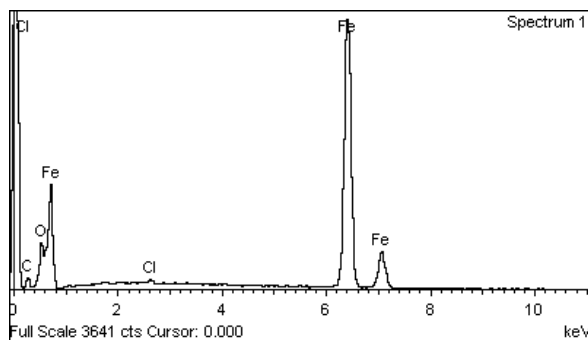


Figure 4. Energy-Dispersive X-ray (EDX) spectrum of the mild steel after corrosion test

3.3. Effect of Temperature on 0.3M AEPD Solution

Fundamentally, during the corrosion rate measurements, anodic reaction held on the steel surface in the corrosion cell; it loses electrons dissolved and releases positively charged ions into the solution while cathodic reaction as the metal releases electron through the electrical circuit. The aqueous solution which contains the water and oxygen molecules mostly received the electron and forming negatively charged hydroxide ions. The positively charged ions will combine with the hydroxide ions and form the corrosion layer on the steel surface. It can be observed that from the results table, that as lower the resistance recorded, the corrosion rate will be higher.

Table 4. Electrochemical parameters extracted from Tafel extrapolation of 0.3M AEPD at different temperature

Temp.	E _{corr} [mV]	I _{corr} [$\mu\text{A}\cdot\text{cm}^{-2}$]	β_a (V/dec)	β_c (V/dec)	R _p [Ωcm^2]	CR [mmPY] $\times 10^{-3}$
50°C	-348.501	0.36880	0.206	0.089	733.9	7.948
70°C	-183.812	0.705431	0.075	0.052	1901	15.203
90°C	-177.858	1.68334	0.144	0.078	1299	36.261

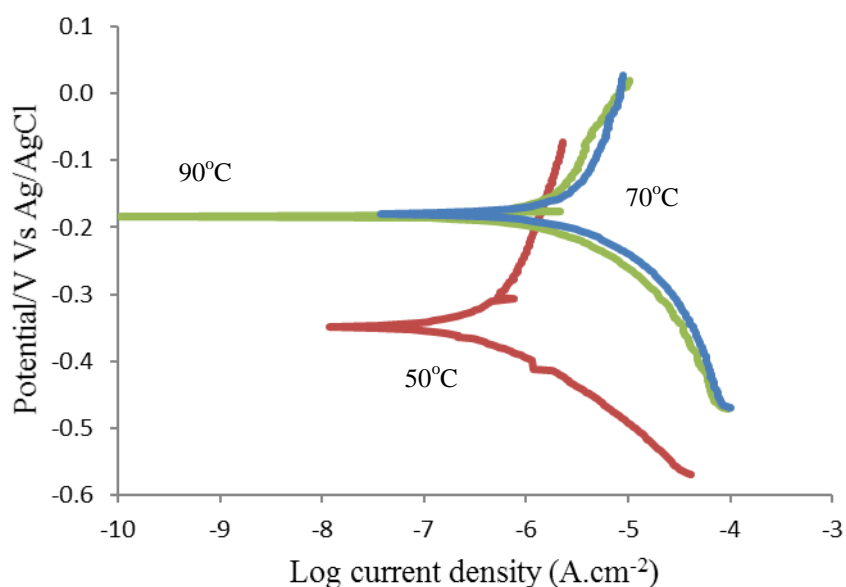


Figure 5. Tafel curves of A36 mild steel electrode in 0.3 of APED at 50, 70, 90°C

This might be justified by the higher transfer rate of electron throughout the reaction, higher combination rate of Fe^{2+} and OH^- to form ferrous hydroxide, $\text{Fe}(\text{OH})_2$. Later on, the ferrous hydroxide will be oxidized to ferric salt as mentioned in equation 3-6. The half reaction for anodic is the oxidation of iron to ferrous ion:



For cathodic reaction is the reduction of hydroxyl ion to O_2 and H_2O



Formation of corrosion product is the iron(II) hydroxide



Later on, iron (II) hydroxide will be oxidized and form iron(III) hydroxide, or ferric salt.



The Tafel Plots for the mild steel in aqueous of AEPD 0.3M was measured at 50°C, 70°C, and 90°C temperatures and presented in Figure 5. The Tafel plots were obtained at the potential range from -250 to +250 mV at a scan rate of 10 mV/minute and I Range (A) of 5 A. The kinetic parameters including corrosion current density, I_{corr} and corrosion rate are given in Table 4.

The Tafel plots showed positive display and appropriate trending for all the parameters, as the temperature of the aqueous AEPD increase, it showed a higher slope on the current recorded for the cathodic part, for 50, 70, and 90°C respectively. Corrosion rate directly depends on the temperature of the amine solution, many side reactions took place such as solvent degradation, the formation of stable salts and high corrosion rate are prominent at a higher temperature [46]. The formation of oxide leads to passivation on the exposed area of the metal, the further corrosion is decreased and decrease in corrosion current to be recorded on the Tafel plot and this has happened on the cathodic current part. The effect of dissolved oxygen on the cathodic kinetics is also considered the decreased diffusion thickness and increased diffusion coefficient [47]. However, according to the corrosion principal, as temperature increases, the corrosion rate also increased. As the dissolved oxygen, and hydroxide enhances the reduction rate, it combines and forms the metal oxide on the exposed area of the steel at a higher rate. The result for temperature aspect follows as increasing temperature, the corrosion rate yielded at about 7.498×10^{-3} mm/year, 15.203×10^{-3} mm/year, and 36.261×10^{-3} mm/year, for the 50, 70, and 90°C respectively.

3.4. Effect of Concentration on AEPD

The Tafel plots for the mild steel in aqueous solutions of AEPD with three concentrations (0.3, 0.6, and 0.9M) were measured at 50°C of and illustrate in Figure 6. The pattern of Tafel graphs is almost the same for all the concentration. As the temperature is maintained at 50°C, the increase of concentration results in a steeper slope for the upper part of the current recorded. It may be as a result of the passivation layer that is developed on the metal steel sample. As passivation layer is formed, the corrosion effect that is supposed to take place begins to slow down, displayed a steep slope at the upper part of the cathodic current. It means, the corrosion taking place at the metal has lowered down, and less current recording (even though the voltage increase). An unusual pattern is observed at the 0.6 M concentration as it yielded a lower corrosion rate than the 0.3 M, most probably to the quick formation of the passivation layer onto the metal surface. Two different corrosion performances are realized due to the variations of amine concentration. These results are agreed with Veawab et. al., [48], reported that corrosion rate is accelerated by increasing the amine concentration and the corrosion rate decreased progressively as the concentration of amine increased. After all, increasing the concentration of the solutions yielded a higher rate of corrosion. This is due to the higher amounts of protonated ion which later on combine with the bicarbonate anion to produce iron carbonate on the

exposed steel area. The result for concentration factor follows as increasing temperature, the corrosion rate yielded at about 7.498×10^{-3} mm/year, 1.980×10^{-3} mm/year, and 35.867×10^{-3} mm/year, for the 50, 70, and 90°C respectively as given in Table 5. Sterically hindered amines solutions were less destructive than MEA due to the thin loadings the corrosion rate was much lower [49].

Table 5. Electrochemical parameters extracted from Tafel extrapolation of AEPD at 50°C

Conc.	E_{corr} [mV]	I_{corr} [$\mu\text{A}\cdot\text{cm}^{-2}$]	β_a (V/dec)	β_c (V/dec)	R_p [Ωcm^2]	CR [mmPY] $\times 10^{-3}$
0.3 M	-348.501	0.36880	0.206	0.089	733.9	7.498
0.6 M	-245.304	0.09188	0.125	0.052	1724	1.980
0.9 M	-380.607	1.664	0.456	0.158	3059	35.867

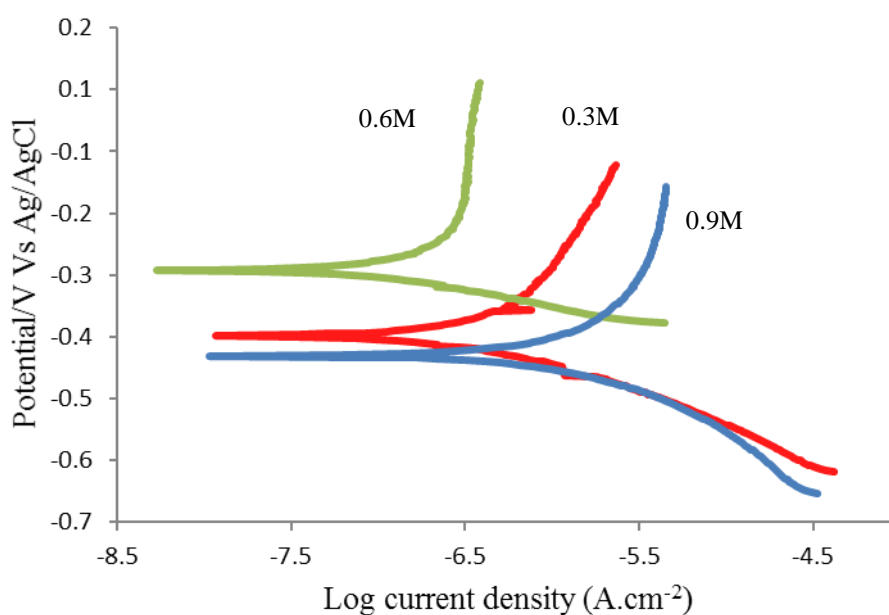


Figure 6. Tafel curves of A36 mild steel electrode in 0.3, 0.6, 0.9M of APED at 50°C

3.5. Potentiodynamic Curves

Potentiodynamic curves for the mild steel in aqueous AEPD were measured with 0.9M under two temperatures 50 and 70°C as showed in Figure 7 and corrosion rates are mentioned in Table 6. For the potentiodynamic method, both curves concerning to the temperature of 50 and 70°C respectively, showed the similar trend in the region where the metal sample corrodes, as the applied potential is more positive. The passivation starts at the point where the cathodic current starts. Passivation is probably due to the formation of a film on the surface on the steel. At the point where the slope is high approaching vertical lines for both graphs, displayed the decrease in the current rapidly, as the passivating film forms on the steel sample. At the region where the current starts to increase back, the passivating film begins to break down in that period, known as the transpassive region, where oxygen evolution starts to occur. After all, from both curves yielded high corrosion rate, due to the high

concentration 0.9M and temperature. At 70°C, 0.9M solution yielded much higher corrosion rate that is 197.880×10^{-3} mm/year, while the at 50°C 0.9M solution yielded lower corrosion rate which is 115.51×10^{-3} mm/year. The overall potentiodynamic technique shows a good trend on the high concentration of amine solution for the corrosion cell at 50 and 70 °C, at 0.9 M concentration. These results are agreed with Rashidi and Valeh-e-Sheyda [50], as they reported that corrosion rate was increased by increasing the concentration of amine solution in regular exposure of the fresh metal surface to the corrosive environment.

Table 6. Corrosion rate for Potentiodynamic of 0.9M APED at 50 and 70 °C)

Temp.	E _{corr} [mV]	I _{corr} [μ A.cm ⁻²]	β_a (V/dec)	β_c (V/dec)	R _p [Ω cm ²]	CR [mmPY] $\times 10^{-3}$
50°C	-416.585	5.360	1.898	0.242	1741.2	115.505
70 °C	-362.795	9.182	0.256	0.175	4912	197.880

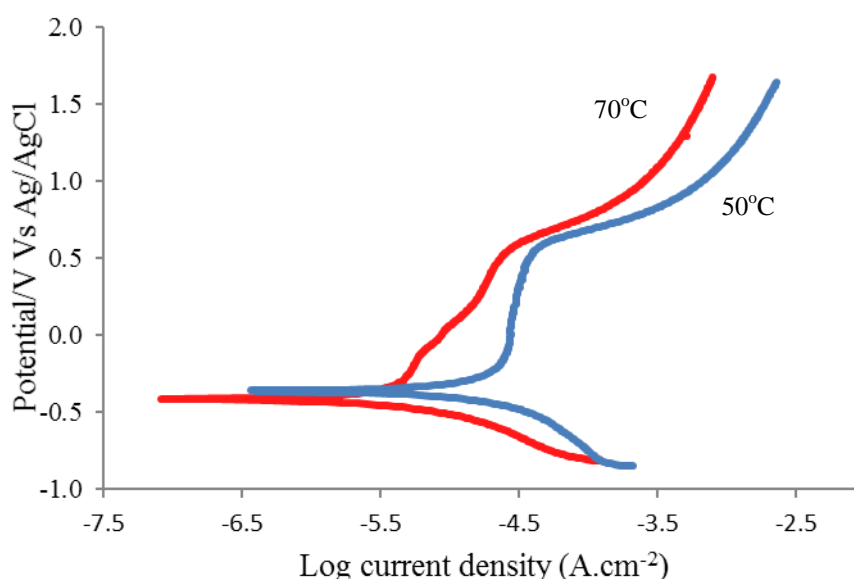


Figure 7. Potentiodynamic curves of aqueous APED 0.9M at 50 and 70 °C

3.6. Effect of Concentration on DEA

It is desirable to analyze and compare the results between the conventional alkanolamines (DEA) and the sterically hindered amines (AEPD). The Tafel plots for the mild steel in aqueous Diethanolamine (DEA) were measured in 0.3, 0.6, and 0.9 M at 50 °C and presented in Figure 8 and electrochemical measurements are illustrated in Table 7. For the Tafel plots, trends obtained are better in the corrosion rate, by means that, all three curves shown a pattern of signifying tendencies to corrode at higher rates. The cathodic part of the plot did not really describe the passivation pattern, but to stress on, for the 0.9 M of DEA concentration, it clearly recorded the highest corrosion rate at 337.721×10^{-3} mm/year. This is due to the high concentration of the DEA itself, which promotes to a system that corroded the steel well. The corrosion rates are followed by 65.146×10^{-3} mm/year, and 24.704×10^{-3} mm/year, for 0.6 and 0.3M concentration, respectively. Overall, it follows that the higher

the concentration of amine, in this case of DEA, the higher the corrosion rates obtained. Veawab et. al. [49] deliberated the corrosion and corrosion inhibition in a sterically hindered amine, 2-amino-2-methyl-1-propanol (AMP), by weight loss method and results were compared with a monoethanolamine (MEA) , which was concurrently certified in the similar environments. They reported that the AMP was normally less corrosive to carbon steel compare to the MEA, however corrosion control is still required.

Table 7. Electrochemical parameters extracted from Tafel extrapolation of DEA at 50°C

Conc.	E _{corr} [mV]	I _{corr} [$\mu\text{A}\cdot\text{cm}^{-2}$]	β_a (V/dec)	β_c (V/dec)	R _p [Ωcm^2]	CR [mmPY] $\times 10^{-3}$
0.3 M	-231.57	1.150	0.013	0.067	1650.4	24.704
0.6 M	-223.49	2.855	0.208	0.102	1042.8	65.146
0.9 M	-92.35	15.67	0.153	0.172	224.4	337.721

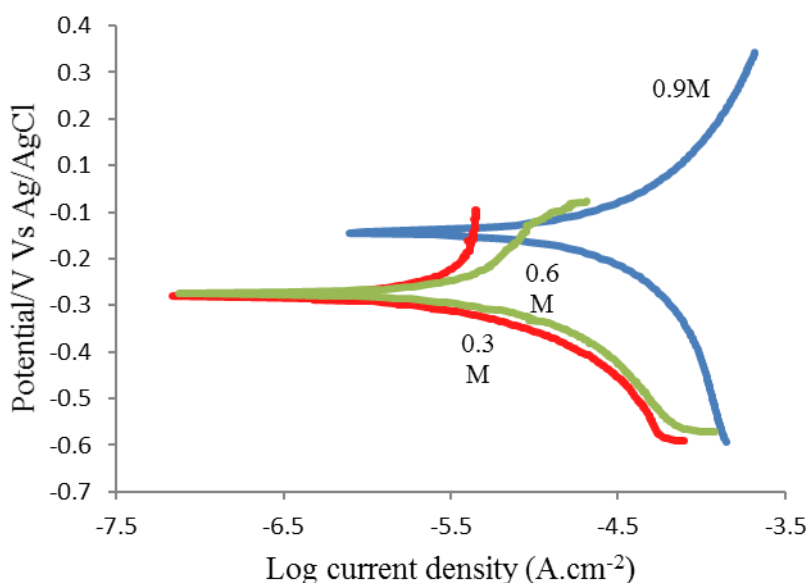


Figure 8. Tafel curve of A36 mild steel electrode in aqueous DEA, 0.3, 0.6, 0.9M at 50°C

3.7. Mixture of AEPD and DEA (0.3, 0.6, 0.9 M)

The Tafel Plots for the mild steel in aqueous mixture 0.3, 0.6, and 0.9M of AEPD and DEA were measured at 50°C and illustrated in Figure 9 and corrosion rates are presented in Table 8. From the Tafel plots, the trends obtained are similar to the previous trending happened on the concentration and temperature, parameters. They consist of the passivation patterns at the cathodic current, plus with the higher corrosion rate yielded for every concentration increment. In this parameter, the corrosion rate yielded for 0.3 M was recorded as 19.024×10^{-3} mm/year. As compared to the previous results (concentration and temperature), it showed a higher rate. The same results also occurred on the 0.6 and 0.9M, respectively.

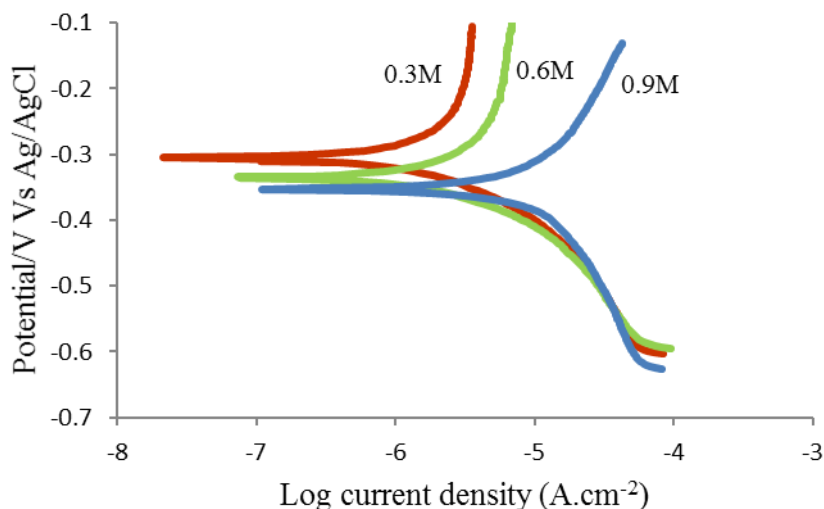


Figure 9. Tafel curve of A36 mild steel electrode in blended mixture of AEPD and DEA at 50°C

As compared to the previous results, for the blended amines, 0.6M concentration yielded much higher rate at 52.920×10^{-3} mm/year. Meanwhile, for the 0.9M concentration, it showed a much higher rate at 119.115×10^{-3} mm/year. The higher rates obtained for all the concentrations of the mixed amines are due to the existence of the DEA in the solutions. Even though DEA is rather used in the industry as the solvent in the CO₂ absorption in gas sweetening plant, it still possesses the ability to yield a higher corrosion rate.

Table 8. Electrochemical parameters extracted from Tafel extrapolation for blended mixture of AEPD and DEA at 50°C

Conc.	E _{corr} [mV]	I _{corr} [μ A.cm ⁻²]	β_a (V/dec)	β_c (V/dec)	R _p [Ω cm ²]	CR [mmPY] $\times 10^{-3}$
0.3 M	-255.518	0.882.735	0.1	0.064	1920.3	19.024
0.6 M	-285.978	2.456	0.228	0.107	1286.4	52.920
0.9 M	-303.071	5.527	0.116	0.089	395.9	119.115

4. CONCLUSION

The corrosion of 2- amino-2-ethyl-1, 3-propanediol (AEPD) and Diethanolamine (DEA) towards A36 mild steel have been investigated through weight loss method. FESEM and EDX analysis showed the steel structure is destroyed by the formation of corrosion products on the surface. From the analysis, different components like iron, oxygen, and chloride were identified on the surface of samples due to the formation of corrosion products. It was found that corrosion rate increased with increasing temperature. This increase in temperature causes to combine the increasing rate of dissolved oxygen and hydroxide that directly enhanced the reduction rate. It combines to forms the metal oxide on the exposed area of the steel at a higher rate. The highest rate for this factor was found to be 36.261×10^{-3} mm/year with a concentration of 0.3M AEPD at 90°C. The corrosion rate was also found to be increased with increasing oxygen concentration. This is caused due to an increase in the

dissolved oxygen present in the tested solution. The higher rate of ferrous hydroxide and ferric salt (rust) on the steel with the concentration of 0.9M AEPD and corrosion rate was observed 35.867×10^{-3} mm/year and found to be boost up its yield. Highest corrosion rate 337.721×10^{-3} mm/year was obtained using 0.9M DEA at 50°C. The corrosion rate of a mixture of AEPD and DEA solution was noted to be low than DEA solution. It can be concluded that satirically hindered amines, specifically, AEPD shows a low corrosion rate yield that regarded as one of the promising candidate of CO₂ absorption solvent for future. The highest yield of a mixture of AEPD and DEA was observed 119.115×10^{-3} mm/year with 0.9M.

ACKNOWLEDGEMENT

This work was financially supported Research Centre for CO₂ Capture (RCCO2C), Universiti Teknologi PETRONAS.

References

1. A. Samanta, A. Zhao, G.K. Shimizu, P. Sarkar, R. Gupta, *Ind. Eng. Chem. Res.*, 51 (2011) 1438-1463.
2. C.C. Cormos, *Int. J. Hydrogen Energy.*, 36(2011) 3726-3738.
3. W.M. Budzianowski, *Int J Global Warm.*, 7 (2015) 184-225.
4. Q.-Y. Wang, X.-Z. Wang, H. Luo, J.-L. Luo, *Surf. Coat. Technol.*, 291 (2016) 250-257.
5. M.F. Morks, P. Corrigan, N. Birbilis, I.S. Cole, *Surf. Coat. Technol.*, 210 (2012) 183-189.
6. F. Shakerian, K.-H. Kim, J.E. Szulejko, J.-W. Park, *Appl. Energy*, 148 (2015) 10-22.
7. M. Rabensteiner, G. Kingler, M. Koller, G. Gronald, C. Hochenauer, *Int. J. Greenhouse Gas Control*, 39 (2015) 79-90.
8. J. Gao, S. Wang, C. Sun, B. Zhao, C. Chen, *Ind. Eng. Chem. Res.*, 51 (2012) 6714-6721.
9. P.C. Rooney, M. DuPart, *Corros. 2000*, NACE International, 2000.
10. B. Zhao, Y. Sun, Y. Yuan, J. Gao, S. Wang, Y. Zhuo, C. Chen, *Energy Procedia*, 4 (2011) 93-100.
11. M. Hasib-ur-Rahman, H. Bouteldja, P. Fongarland, M. Siaj, F.ç. Larachi, *Ind. Eng. Chem. Res.*, 51 (2012) 8711-8718.
12. M. Desimone, G. Gordillo, S. Simison, *Corros. Sci.*, 53 (2011) 4033-4043.
13. M. Migahed, A. Attia, R. Habib, *RSC Adv.*, 5 (2015) 57254-57262.
14. Y. Xiang, M. Yan, Y.-S. Choi, D. Young, S. Nestic, *Int. J. Greenhouse Gas Control*, 30 (2014) 125-132.
15. L. Zheng, J. Landon, N.S. Matin, G.A. Thomas, K. Liu, *Corros. Sci.*, 106(2016) 281-292.
16. Y.-S. Choi, D. Duan, S. Jiang, S. Nešić, *Corros.*, 69 (2013) 551-559.
17. F. Bougie, M.C. Iliuta, *J. Chem. Eng. Data*, 57 (2012) 635-669.
18. H.H. Khoo, R.B. Tan, *Energy Fuels*, 20 (2006) 1914-1924.
19. L. Zheng, N.S. Matin, J. Landon, G.A. Thomas, K. Liu, *Corros. Sci.*, 102 (2016) 44-54.
20. P. Luis, *Desalin.*, 380 (2016) 93-99.
21. L. Shahhosseini, M.R. Nateghi, S. SheikhSivandi, *Synth. Met.*, 211 (2016) 66-74.
22. J. Gao, L. Cao, H. Dong, X. Zhang, S. Zhang, *Appl. Energy*, 154 (2015) 771-780.
23. S. Ullah, M.A. Bustam, A.M. Shariff, G. Gonfa, K. Izzat, *Appl. Surf. Sci.*, 365 (2016) 76-83.
24. G. Murshid, A.M. Shariff, L.K. Keong, M.A. Bustam, *J. Chem. Eng. Data*, 56 (2011) 2660-2663.
25. P. Narute, G.R. Rao, S. Misra, A. Palanisamy, *Prog. Org. Coat.*, 88 (2015) 316-324.
26. B. Narayanasamy, S. Rajendran, *Prog. Org. Coat.*, 67 (2010) 246-254.
27. A. Madhan Kumar, Z.M. Gasem, *Prog. Org. Coat.*, 78 (2015) 387-394.

28. A.J. Reynolds, T.V. Verheyen, S.B. Adeloju, E. Meuleman, P. Feron, *Environ. Sci. Technol.*, 46 (2012) 3643-3654.
29. M.N. Kakaei, J. Neshati, H. Hoseiny, T. Poursaberi, *Corros. Sci.*, 104 (2016) 132-143.
30. S. Ullah, A.M. Shariff, M. Nadeem, M. A. Bustam, S. A. Shahid, G. Murshid, M. Y. Naz, M. Sagir, M. Mushtaq, *Appl. Mech. Mater.*, 699 (2015) 186-191.
31. S. Ullah, A.M. Shariff, M.A. Bustam, M. Nadeem, M.Y. Naz, M. Ayoub, *Int. J. Electrochem. Sci.*, 10 (2015) 8321 - 8333.
32. I.S. Molchan, G.E. Thompson, P. Skeldon, R. Lindsay, J. Walton, E. Kouvelos, G.E. Romanos, P. Falaras, A.G. Kontos, M. Arfanis, E. Siranidi, L.F. Zubeir, M.C. Kroon, J. Klockner, B. Iliev, T.J.S. Schubert, *RSC Adv.*, 5 (2015) 35181-35194.
33. M. Shokouhi, H. Bozorgzade, P. Sattari, *J. Chem. Eng. Data*, 60 (2015) 2119-2127.
34. P.V. Kortunov, M. Siskin, M. Paccagnini, H. Thomann, *Energy Fuels*, (2016).
35. M. Ozkutlu, O.Y. Orhan, H.Y. Ersan, E. Alper, *Chem. Eng. Process. Process Intensif.*, 101 (2016) 50-55.
36. J.G.-S. Monteiro, H. Knuutila, N.J. Penders-van Elk, G. Versteeg, H.F. Svendsen, *Chem. Eng. Sci.*, 127 (2015) 1-12.
37. T. Supap, R. Idem, P. Tontiwachwuthikul, C. Saiwan, *Ind. Eng. Chem. Res.*, 45 (2006) 2437-2451.
38. J. Lu, L. Wang, X. Sun, J. Li, X. Liu, *Ind. Eng. Chem. Res.*, 44 (2005) 9230-9238.
39. S. Ullah, M. Nadeem, A.M. Shariff, F. Ahmad, S.A. Shahid, M. Sagir, M.R.R. Malik, M. Mushtaq, *Adv. Mater. Res.*, 917 (2014) 28-34.
40. U. Pischel, X. Zhang, B. Hellrung, E. Haselbach, P.-A. Muller, W.M. Nau, *J. Am. Chem. Soc.*, 122 (2000) 2027-2034.
41. Z. Cui, A. Aroonwilas, A. Veawab, *Ind. Eng. Chem. Res.*, 49 (2010) 12576-12586.
42. F. Bougie, M.C. Iliuta, *Ind. Eng. Chem. Res.*, 49 (2009) 1150-1159.
43. A. Veawab, P. Tontiwachwuthikul, A. Chakma, *Ind. Eng. Chem. Res.*, 38 (1999) 310-315.
44. E.B. Rinker, S.S. Ashour, O.C. Sandall, *Ind. Eng. Chem. Res.*, 39 (2000) 4346-4356.
45. P. Wattanaphan, T. Sema, R. Idem, Z. Liang, P. Tontiwachwuthikul, *Int. J. Greenhouse Gas Control*, 19 (2013) 340-349.
46. H. Rashid, N. Hasan, M.I. Mohamad Nor, *Chem. Prod. Process Model.*, 2014, pp. 105.
47. J. Li, B. Hurley and R. Buchheit, *J. Electrochem. Soc.*, 162(6) (2015) C219-C227.
48. A. Veawab, P. Tontiwachwuthikul, A. Chakma, *Ind. Eng. Chem. Res.*, 38 (1999) 3917-3924.
49. A. Veawab, P. Tontiwachwuthikul, S.D. Bhole, *Ind. Eng. Chem. Res.*, 36 (1997) 264-269.
50. H. Rashidi, P. Valeh-e-Sheyda, *Int. J. Greenhouse Gas Control*, 47 (2016) 101-109.